

Electron distribution in the $\text{Cr}(\text{CO})_4(\text{bpy})^{\cdot-}$ (bpy = 2,2'-bipyridine) radical anion as revealed by EPR spectroscopy and IR spectro-electrochemistry of ^{13}C -enriched species

Antonín Vlček, Jr.,^{*,a,b} Frank Baumann,^c Wolfgang Kaim,^c Friedrich-Wilhelm Grevels^d and František Hartl^c

^a Department of Chemistry, Queen Mary and Westfield College, London, UK E1 4NS

^b J. Heyrovský Institute of Physical Chemistry, Academy of Sciences of the Czech Republic, Dolejškova 3, CZ-182 23 Prague, Czech Republic

^c Institut für Anorganische Chemie, Universität Stuttgart, Pfaffenwaldring 55, D-70550 Stuttgart, Germany

^d Max-Planck-Institut für Strahlenchemie, Postfach 101365, D-45413, Mülheim a.d. Rhur, Germany

^e Anorganisch Chemisch Laboratorium, J.H. van't Hoff Research Instituut, Universiteit van Amsterdam, Nieuwe Achtergracht 166, NL-1018 WV, Amsterdam, The Netherlands

Samples of $\text{Cr}(\text{CO})_4(\text{bpy})$ (bpy = 2,2'-bipyridine) with natural abundance of ^{13}C and with 16 and 79% ^{13}C enrichment, respectively, were reduced to the corresponding radical anion, $[\text{Cr}(\text{CO})_4(\text{bpy})]^{\cdot-}$ and studied by EPR and IR spectroscopies. Electron paramagnetic resonance showed a considerable coupling of the unpaired electron with $^{13}\text{C}(\text{CO})$ of 0.601 mT which occurs to the ^{13}C ligands bound in axial positions, *i.e. cis* to bpy. It indicates an interaction between the singly occupied π^* orbital of the $\text{bpy}^{\cdot-}$ ligand and the σ and/or σ^* orbitals of the axial C–Cr–C bonds. Coupling to the ^{53}Cr nucleus is rather small, 0.128 mT. Infrared spectra in the $\nu(\text{CO})$ region were used to calculate the CO stretching and interaction force constants within the energy factored CO force field approximation. The stretching force constants of the equatorial and axial CO ligands were found to decrease by 68 and 21 N m^{-1} , respectively, on going from $\text{Cr}(\text{CO})_4(\text{bpy})$ to $[\text{Cr}(\text{CO})_4(\text{bpy})]^{\cdot-}$. It follows that the reduction strengthens significantly the π -back donation to the equatorial (*trans* to bpy) CO ligands.

Transition-metal complexes of radical-anionic ligands¹ attract much attention because of interesting spectroscopic and chemical properties induced by the presence of the unpaired electron,¹ their resemblance to metal to ligand charge transfer, MLCT, excited states,^{2–5} and, also, as potential building blocks for molecular magnetic materials.⁶ Properties and behaviour of such compounds appear to be largely determined by the extent of the unpaired electron's delocalisation from the radical-anionic ligand to the metal.^{1,7–11}

Reduction of *cis*- $\text{Cr}(\text{CO})_4(\text{bpy})$ (bpy = 2,2'-bipyridine) to its radical anion is known^{12–16} to occur without any major change in its structure or composition. The EPR spectrum of the $\text{Na}[\text{Cr}(\text{CO})_4(\text{bpy})]$ ion pair^{15,16} resembles that of the uncoordinated $\text{bpy}^{\cdot-}$ radical anion,^{12,17} indicating clearly that the unpaired electron is localised on the bpy ligand. This conclusion is fully corroborated by the similarity between the UV/VIS spectra^{14–16} of $[\text{Cr}(\text{CO})_4(\text{bpy})]^{\cdot-}$ and free $\text{bpy}^{\cdot-}$. Obviously, the product of the one-electron reduction of $\text{Cr}(\text{CO})_4(\text{bpy})$ may best be formulated as a formally chromium(0) complex with a radical-anionic ligand, $[\text{Cr}(\text{CO})_4(\text{bpy}^{\cdot-})]$. Compared with $\text{Cr}(\text{CO})_4(\text{bpy})$, the radical anion is much more labile toward CO substitution. The reduction of $\text{Cr}(\text{CO})_4(\text{bpy})$ was shown¹⁸ to labilise one of the axial (*cis* to bpy) CO ligands which is readily replaced by PPh_3 to yield *fac*- $[\text{Cr}(\text{CO})_3(\text{PPh}_3)(\text{bpy})]^{\cdot-}$ and, ultimately, *fac*- $\text{Cr}(\text{CO})_3(\text{PPh}_3)(\text{bpy})$ by an electron-transfer-catalysed process. Such an activation of an M–CO bond towards nucleophilic substitution in complexes of radical-anionic ligands appears to be quite a general effect.^{1,8,9,11} Its magnitude has been qualitatively related to the extent of the delocalisation of the unpaired electron onto the metal atom.^{8,9,11}

The parent $\text{Cr}(\text{CO})_4(\text{bpy})$ complex has recently attracted

much interest as a prototypical organometallic compound which undergoes very fast, presumably subpicosecond, dissociation of the axial CO ligand upon Cr→bpy MLCT excitation.^{14,19–24} Obviously, there is a similarity² between the chemical effects of MLCT excitation and reduction of $\text{Cr}(\text{CO})_4(\text{bpy})$. Moreover, the visible absorption spectrum of the MLCT excited state of $\text{Cr}(\text{CO})_4(\text{bpy})$ resembles closely that of $[\text{Cr}(\text{CO})_4(\text{bpy})]^{\cdot-}$, suggesting¹⁴ that both species possess the same chromophore, $\text{bpy}^{\cdot-}$. The $\text{Cr}(\text{CO})_4(\text{bpy})$ complex thus provides a very good example of a more general parallelism² between the MLCT excited states and one-electron reduced forms of organometallic and co-ordination compounds.

The relative simplicity of $\text{Cr}(\text{CO})_4(\text{bpy})$ and its radical anion allowed us to perform detailed spectroscopic^{14,23,24} as well as theoretical²⁵ studies which are expected to reveal the MLCT excited state dynamics and the intimate mechanism of the M–CO bond labilisation on MLCT excitation. Herein, we have concentrated on EPR and IR studies of the $[\text{Cr}(\text{CO})_4(\text{bpy})]^{\cdot-}$ radical anion and its ^{13}C -enriched isotopomers. The EPR spectrum of $[\text{Cr}(\text{CO})_4(\text{bpy})]^{\cdot-}$ is, for the first time, fully analysed and all the relevant hyperfine splitting coupling constants determined. Notably, the hitherto unreported hyperfine splitting from ^{53}Cr and $^{13}\text{C}(\text{CO})$ nuclei is determined. The IR spectra in the $\nu(\text{CO})$ region enabled us to calculate all CO stretching and interaction force constants within the energy factored force field, EFFF, approximation.^{26–30} The combined EPR and IR spectroscopic evidence provides information on the delocalisation of the unpaired electron and on the overall changes in the electron density distribution upon the reduction, respectively. Comparison of these complementary data reveal the effects of reduction on the bonding and charge distribution in $\text{Cr}(\text{CO})_4(\text{bpy})$.

Table 1 Isotopic compositions of the ^{13}C -enriched samples of $\text{Cr}(\text{CO})_4(\text{bpy})$ as calculated from the total enrichments determined by mass spectrometry^{*32}

$n(^{13}\text{C})$	79% Enrichment				16% Enrichment			
	Total	0ax	1ax	2ax	Total	0ax	1ax	2ax
0	0.2	0.2	0.0	0.0	49.8	49.8	0.0	0.0
1	2.9	1.5	1.5	0.0	37.9	18.9	18.9	0.0
2	16.5	2.8	11.0	2.8	10.8	1.8	7.2	1.8
3	41.4	0.0	20.7	20.7	1.4	0.0	0.7	0.7
4	39.0	0.0	0.0	39.0	0.1	0.0	0.0	0.1
Total	100.0	4.5	33.2	62.5	100.0	70.5	26.8	2.6

* Individual columns show the total percentage of the isotopomers with n ^{13}C ligands and the percentage of the isotopomers which have 0, 1 or 2 ^{13}C ligands in the axial positions.

Experimental

The samples of $\text{Cr}(\text{CO})_4(\text{bpy})$ with a natural abundance of ^{13}C and with ^{13}C -enrichment were prepared by the method of Stiddard³¹ and purified by recrystallisation from a CH_2Cl_2 -2,2,4-trimethylpentane mixture under a nitrogen atmosphere. Tetrahydrofuran (THF) (Merck) was distilled from a sodium-benzophenone mixture under nitrogen before use. Tetra-*n*-hexylammonium hexafluorophosphate (THAPF_6) was obtained from Professor A. M. Bond, Deakin University (Australia).

Electron paramagnetic resonance measurements were performed at 295 K using a Bruker ESP 300 instrument at 9.8504 GHz. Modulation amplitude of 0.002 mT and microwave power of 1.5 mW were used. The radical anions were generated by reduction of individual samples of $\text{Cr}(\text{CO})_4(\text{bpy})$ in THF on a potassium mirror under high vacuum. The solutions contained an excess of Merck Kryptofix 222, *i.e.* 4,7,13,16,21,24-hexaoxo-1,10-diazabicyclo[8.8.8]hexacosane, hereinafter referred to as cryptand. Reduced solutions were transferred into a capillary which was then sealed off under vacuum. The radical anion $[\text{Cr}(\text{CO})_3(\text{PBU}^n_3)(\text{bpy})]^-$ was generated by the same procedure in the presence of an excess of PBU^n_3 .

Computer simulations were performed using standard adapted EPR simulation software. Gaussian line forms were assumed and no corrections have been made for second-order or variable line-width effects. The first simulation did not include any ^{13}C coupling, the second was performed with one additional ^{13}C nucleus and the third with two equivalent ^{13}C nuclei. The simulated EPR spectrum of the 79% ^{13}C -enriched $[\text{Cr}(\text{CO})_4(\text{bpy})]^-$ was obtained as a sum of these three spectra in an approximate ratio of the abundances of corresponding isotopomers, calculated from the mass spectra, Table 1.

Infrared spectroelectrochemical experiments were performed *in situ* by reducing degassed THF solutions of individual samples of $\text{Cr}(\text{CO})_4(\text{bpy})$ on a Pt mesh electrode within the low-temperature IR optically transparent thin layer electrochemical (LT-OTTLE) cell³³ cooled to -32°C . A PA-4 Ekom potentiostat was employed; 0.1 M THAPF_6 was used as an electrolyte. Infrared spectra were measured on a Bio-Rad FTS-7 FTIR instrument with a resolution of 2 cm^{-1} . The CO stretching force constants and the composition of vibrational normal modes were calculated as described in ref. 32. A reduced mass ratio of 0.978 13 was used in the calculations.

Results

The $\text{Cr}(\text{CO})_4(\text{bpy})$ molecule is schematically shown in Fig. 1. Spectroscopic studies were performed on a $\text{Cr}(\text{CO})_4(\text{bpy})$ sample with a natural isotopic distribution and on two samples³² enriched with ^{13}C to 16 or 79%, respectively, as was determined by mass spectrometry.³² Mass spectra have indicated

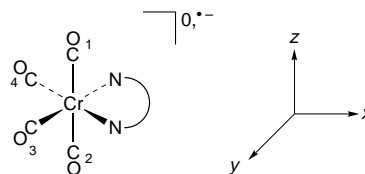


Fig. 1 Schematic structures of $\text{Cr}(\text{CO})_4(\text{bpy})$ and $[\text{Cr}(\text{CO})_4(\text{bpy})]^-$, labelling of the CO ligands and chosen orientation of the axes. Axial CO ligands 1,2 lie above and below the $\text{Cr}(\text{bpy})$, xy , plane, equatorial ones 3,4 lie within this plane

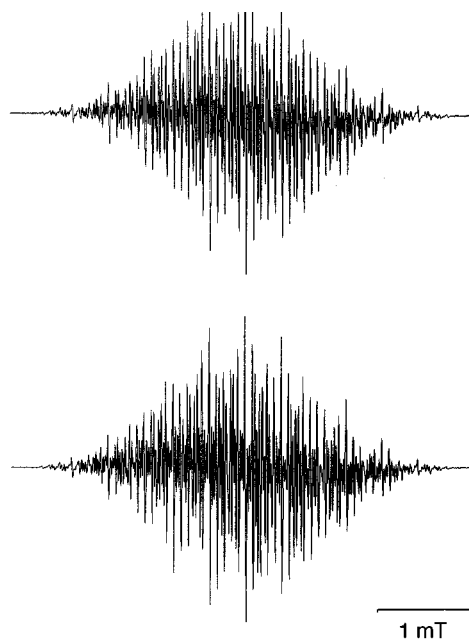


Fig. 2 Experimental (top, THF, 295 K) and simulated (bottom) EPR spectra of $[\text{Cr}(\text{CO})_4(\text{bpy})]^-$ enriched with ^{13}C to 79% (line width 0.013 mT; see text for further information)

statistical distribution of individual isotopomers in both enriched samples.³² Corresponding abundances are summarised in Table 1.

EPR Spectra

Electron paramagnetic resonance spectra of $[\text{Cr}(\text{CO})_4(\text{bpy})]^-$ with different degrees of ^{13}C -enrichment were measured in the presence of the cryptand. The formation of the bulky $[\text{K}(\text{cryptand})]^+$ counter cation is assumed to avoid any ion-pairing effects. The spectra are centred at an isotropic g value of 2.0026. The spectrum of the non-enriched sample may be analysed in terms of the hyperfine splitting, hfs, from four distinct pairs of equivalent ^1H ($I = \frac{1}{2}$) nuclei and from two equivalent ^{14}N ($I = 1$) nuclei of the bpy ligand. Moreover, hfs from the ^{53}Cr nucleus ($I = \frac{3}{2}$, 9.54%) was resolved at the outermost section of the spectrum. The following coupling constants were obtained by computer simulation:† $a(\text{H}^{3,3'}) = 0.105$, $a(\text{H}^{4,4'}) = 0.124$, $a(\text{H}^{5,5'}) = 0.451$, $a(\text{H}^{6,6'}) = 0.075$, $a(\text{N}) = 0.371$, $a(^{53}\text{Cr}) = 0.128$ mT. The same hfs pattern also occurs in the spectra of the two ^{13}C -enriched samples, together with an additional splitting that originates in the hyperfine coupling with the $^{13}\text{C}(\text{CO})$ nuclei ($I = \frac{1}{2}$).

The EPR spectrum of the 79% ^{13}C -enriched $[\text{Cr}(\text{CO})_4(\text{bpy})]^-$ is shown in Fig. 2 (top), together with the corresponding computer-simulated spectrum (bottom). It is interpreted as a superposition of three spectra: (i) one spectrum with no ^{13}C hfs, (ii) one spectrum with hfs from a single ^{13}C

† The hfs values expressed in cm^{-1} are: $a(\text{H}^{3,3'}) = 9.817 \times 10^{-5}$, $a(\text{H}^{4,4'}) = 1.159 \times 10^{-4}$, $a(\text{H}^{5,5'}) = 4.216 \times 10^{-4}$, $a(\text{H}^{6,6'}) = 7.012 \times 10^{-5}$, $a(\text{N}) = 3.469 \times 10^{-4}$, $a(^{53}\text{Cr}) = 1.197 \times 10^{-4}$, $a(^{13}\text{C}) = 5.619 \times 10^{-4}$.

nucleus which splits each line of the ^{12}C -only spectrum into a doublet of equal intensities, and, (iii) one spectrum with hfs from a single pair of two equivalent ^{13}C nuclei which splits the lines of the ^{12}C -only spectrum into 1:2:1 triplets. The values of the ^{13}C coupling constants in the spectra (ii) and (iii) are identical at 0.601 mT. This shows that the ^{13}CO ligands responsible for the hfs in the spectra (ii) and (iii) are located at positions of the same type. They correspond either to the two axial sites (*cis* to bpy) or to the two equatorial sites (*trans* to bpy). It has been amply documented¹ for complexes of the type $[\text{M}(\text{E})(\text{CO})_3(\text{L}^{\cdot-})]$ or $[\text{M}(\text{E})_2(\text{CO})_2(\text{L}^{\cdot-})]$, E = phosphine, arsine, stibine, amine, *etc.*, that the hfs due to the nucleus of the donor atom of the ligand E is much larger if it is located in the axial position, *i.e.* if the M–E bond is perpendicular to the plane of the chelating radical-anionic ligand $\text{L}^{\cdot-}$. Hence, we attribute the $^{13}\text{C}(^{13}\text{CO})$ hfs in ^{13}CO -enriched $[\text{Cr}(\text{CO})_4(\text{bpy})]^{-\cdot}$ to the ^{13}CO ligand(s) bound in the axial position(s). This conclusion is further corroborated by the comparison of the value of $a(^{13}\text{C})$ measured for $[\text{Cr}(\text{CO})_4(\text{bpy})]^{-\cdot}$ and that of $a(^{31}\text{P})$, 3.517 mT, found for the *fac*- $[\text{Cr}(\text{CO})_3(\text{PBU}^n_3)(\text{bpy})]^{-\cdot}$ ion in which the PBU^n_3 ligand is bound^{18,34} at the axial position. The $a(^{13}\text{C})/a(^{31}\text{P})$ ratio of 0.17 is of a comparable magnitude with the $A_{\text{iso}}(^{13}\text{C})/A_{\text{iso}}(^{31}\text{P})$ ratio of 0.29:1 (A_{iso} is an hfs constant calculated^{35,36} for a full localisation of the unpaired electron in the s orbital of a given atom). This indicates not only the same (*i.e.* axial) co-ordination positions of the ^{13}C and ^{31}P nuclei from which the hfs arises but also suggests a similar mechanism of the spin density delocalisation in both anions. Splitting from two non-equivalent ^{13}C nuclei or from more than two ^{13}C nuclei was not found despite the fact that the 79% ^{13}CO -enriched sample is composed mostly of the $[\text{Cr}(^{12}\text{CO})(^{13}\text{CO})_3(\text{bpy})]^{-\cdot}$ and $[\text{Cr}(^{13}\text{CO})_4(\text{bpy})]^{-\cdot}$ isotopomers, see Table 1. This result implies that the ^{13}C hfs from the ^{13}CO ligands bound at the equatorial positions is negligible, much smaller than the EPR linewidth of 0.013 mT.

The overall ^{13}C splitting results in an apparent quintet whose lines are separated by one half of the ^{13}C splitting constant. The relative intensities of the EPR lines may be evaluated from the relative abundances of the isotopomers (Table 1) and from the splitting patterns discussed above. Hence, the intensity of the outermost lines of the quintet is equal to $\frac{1}{4}$ of the abundance of those isotopomers which have two axial ^{13}CO ligands, regardless of the isotopic character of the equatorial CO ligands. The intensity of the inner two lines of the quintet is equal to $\frac{1}{2}$ of the abundance of all the isotopomers which have a single ^{13}CO ligand in an axial position, regardless of the isotopic character of the equatorial CO ligands. Finally, the intensity of the central line is equal to $\frac{1}{2}$ of the total abundance of the isotopomers which have two axial ^{13}CO ligands, plus the abundance of all the isotopomers which contain no axial ^{13}CO ligands. Hence, the intensity ratio of 0.156:0.166:0.358:0.166:0.156 may be calculated for the apparent ^{13}C -quintet of the 79%-enriched sample while a ratio of 0.007:0.134:0.718:0.134:0.007 follows for the sample enriched to 16%. The ^{13}C splitting of the latter sample will be manifested only as the 0.134:0.718:0.134 apparent triplet, since the outermost lines of the apparent quintet are too weak to be observed experimentally. The ^{13}C hfs is best discernible at the sides of the EPR spectra, see Fig. 3. Comparison of the low-field part of the spectrum of the non-enriched $[\text{Cr}(\text{CO})_4(\text{bpy})]^{-\cdot}$ with those of the 16 and 79% enriched species allows us to identify the last line of the ^{12}C -only spectrum. The separations between this line and the last line of the spectra of the samples enriched to 16 and 79% correspond to $a(^{13}\text{C})/2$ and $a(^{13}\text{C})$, respectively. The value measured directly from the spectra, *ca.* 0.6 mT, is identical with that obtained by computer simulation of the full spectrum. The above intensity considerations predict that the intensity of the last line of the spectrum of the 16%-enriched species will be 18.7% of the intensity of the last ^{12}C -only line. The calculated value compares very well with the experimental value of 18%.

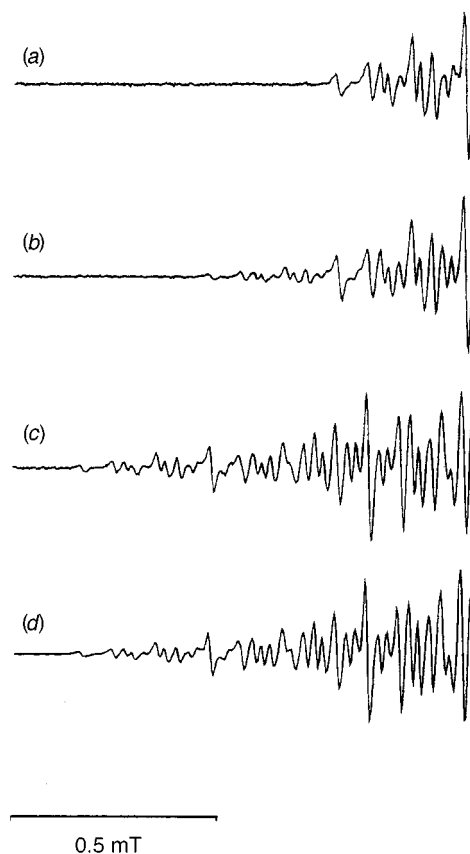


Fig. 3 Low-field sections of EPR spectra of $[\text{Cr}(\text{CO})_4(\text{bpy})]^{-\cdot}$ samples with different extent of ^{13}CO -enrichment, measured in THF at 295 K. From top to bottom: experimental spectra of the natural abundance (a), 16% ^{13}CO -enriched (b), 79% ^{13}CO -enriched (c) samples, and, bottom, the computer simulated spectrum of the 79% ^{13}CO -enriched sample (d)

IR spectroelectrochemistry

The IR spectra of the natural abundance sample and the two ^{13}CO -enriched samples of $\text{Cr}(\text{CO})_4(\text{bpy})$ and of their reduction products, that is of $[\text{Cr}(\text{CO})_4(\text{bpy})]^{-\cdot}$ radical anions with different degrees of ^{13}CO -enrichment, were studied in the $\nu(\text{CO})$ spectral region. Spectra monitored during the electrochemical reduction exhibit well defined isosbestic points. Shown in Fig. 4 are the IR spectra of the three $\text{Cr}(\text{CO})_4(\text{bpy})$ samples before (dashed lines) and after the reduction (solid lines). The IR wavenumbers are summarised in Table 2. Fig. 4 shows that the overall IR spectral pattern and the intensity ratios of the bands hardly change on reduction. Obviously, the C_{2v} symmetry of the natural abundance $\text{Cr}(\text{CO})_4(\text{bpy})$ molecule is retained by its radical anion. Hence, the same four IR-active $\nu(\text{CO})$ vibrations, $2A_1 + B_1 + B_2$, are expected for both species and the IR bands of $[\text{Cr}(\text{CO})_4(\text{bpy})]^{-\cdot}$ may be assigned³² by analogy with $\text{Cr}(\text{CO})_4(\text{bpy})$. Thus, the most intense band is attributed to the B_1 out-of-phase stretching vibration of the axial CO ligands and the lowest-frequency band to the B_2 out-of-phase stretch of the equatorial ones. The highest-frequency band and the second lowest band then belong to the two totally symmetric vibrations, denoted A_1^2 and A_1^1 , respectively.

Comparison of the IR spectra of $\text{Cr}(\text{CO})_4(\text{bpy})$ and its radical anion, Fig. 4, shows the shift of the $\nu(\text{CO})$ modes to lower wavenumbers to be the main effect of the reduction. The magnitude of this shift is less than that observed^{12,37} for metal-centred reduction of carbonyl complexes, in line with the formulation of the anionic complex as $[\text{Cr}(\text{CO})_4(\text{bpy})]^{-\cdot}$. The CO stretching vibrations of $[\text{Cr}(\text{CO})_4(\text{bpy})]^{-\cdot}$ are described, within the energy factored CO force field approximation, EFFF,^{26–30} by five force constants: the stretching force constants of the axial and equatorial CO ligands, denoted k_{ax} and k_{eq} , respectively, and three

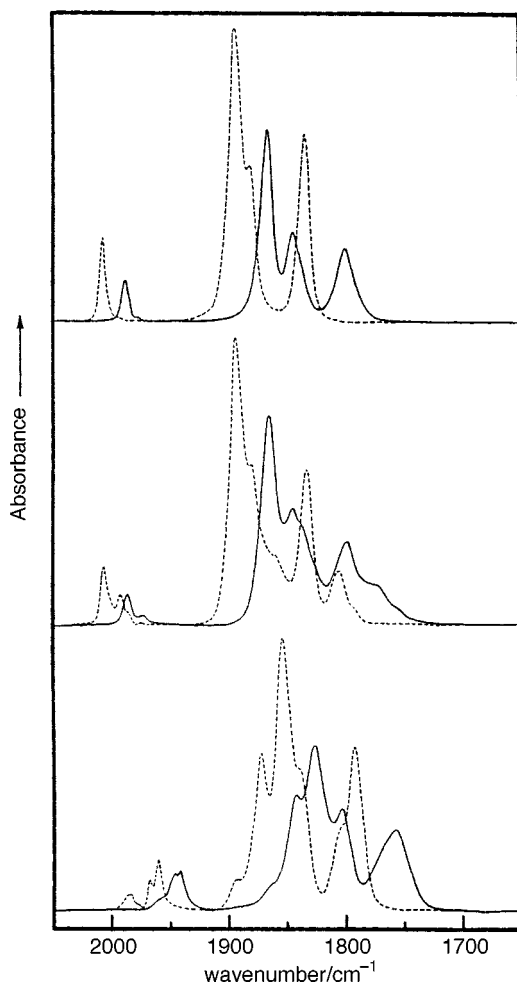


Fig. 4 Infrared spectra of $\text{Cr}(\text{CO})_4(\text{bpy})$ (---) and $[\text{Cr}(\text{CO})_4(\text{bpy})]^{-}$ (—) in THF solutions at 241 K. Top: natural abundance; centre: 16% ^{13}C O-enrichment; bottom: 79% ^{13}C O-enrichment. The spectra of the anion radicals were obtained from the spectra measured after a nearly complete reduction by subtracting the spectra of the traces (*ca.* 5%) of the residual unreduced parent species

interaction constants $k_{\text{ax,ax}}$, $k_{\text{eq,eq}}$ and $k_{\text{ax,eq}}$. They were calculated from the $\nu(\text{CO})$ wavenumbers (Table 2) of $[\text{Cr}(\text{CO})_4(\text{bpy})]^{-}$ and its ^{13}C O-containing isotopomers. Force constants and normal coordinates obtained[‡] are summarised in Tables 3 and 4 and compared with those³² of $\text{Cr}(\text{CO})_4(\text{bpy})$. The match between the experimental $\nu(\text{CO})$ wavenumbers and those calculated for individual isotopomers by the EFFF procedure is excellent, see Table 2 and Fig. 4.

Reduction of the $\text{Cr}(\text{CO})_4(\text{bpy})$ complex also affects the composition of the vibrational normal coordinates, see Table 4. The vibrational coupling between the axial and equatorial CO ligands slightly decreases on going from $\text{Cr}(\text{CO})_4(\text{bpy})$ to $[\text{Cr}(\text{CO})_4(\text{bpy})]^{-}$. Accordingly, the experimental intensity ratio of the IR bands due to the A_1^2 and B_1 modes decreases from *ca.* 0.28 to 0.22.

[‡] It should be noted that deleting the 1836 cm^{-1} band from the input data of the EFFF calculation produces an alternative set of force constants: $k_{\text{ax}} = 1481$, $k_{\text{eq}} = 1362$, $k_{\text{ax,ax}} = 72$, $k_{\text{eq,eq}} = 55$, $k_{\text{ax,eq}} = 43 \text{ N m}^{-1}$, while $Q(A_1^2) = 0.636(r_1 + r_2) + 0.309(r_3 + r_4)$. This solution was rejected because: (i) the band at 1836 cm^{-1} was reliably identified in the spectrum, (ii) the fit between the experimental and calculated wavenumbers is somewhat worse than that presented in Table 1, and (iii) EFFF calculation based on still smaller sets of input data afford solutions very similar to that shown in Table 3. Nevertheless, the qualitative conclusions from the EFFF analysis do not depend on the set of force constants chosen since the alternative solution still indicates that the reduction affects the equatorial CO ligands much more than the axial ones, decreasing the corresponding stretching force constants by 53 and 34 N m^{-1} , respectively.

Table 2 Experimental (THF, 241 K) and EFFF-calculated $\nu(\text{CO})$ wavenumbers (cm^{-1}) of $[\text{Cr}(\text{CO})_4(\text{bpy})]^{-}$ ^a

Isotopomer		A_1^2	B_1	A_1^1	B_2
All ^{12}C O	Exptl.	1988	1868	1845	1799
	Calc.	1988.1	1867.7	1844.9	1799.2
ax	Exptl.	(1972)	—	1836 ^b	1799
	Calc.	1971.8	1850.5	1836.3	1799.2
eq	Exptl.	—	1868	—	1773
	Calc.	1986.4	1867.7	1833.2	1772.6
ax,eq	Exptl.	—	—	—	—
	Calc.	1969.8	1846.5	1829.1	1772.4
ax,ax	Exptl.	—	—	1827	1799
	Calc.	1950.0	1839.7	1826.8	1799.2
eq,eq	Exptl.	—	1868	—	1760
	Calc.	1984.9	1867.7	1807.5	1759.9
ax,eq,eq	Exptl.	—	1843	(1805)	1760
	Calc.	1968.0	1844.6	1805.4	1759.9
ax,ax,eq	Exptl.	—	—	1827	—
	Calc.	1947.3	1829.4	1826.8	1772.3
All ^{13}C O	Exptl.	(1945)	1827	(1805)	1760
	Calc.	1944.6	1826.8	1804.5	1759.9

^a The first column specifies the positions substituted with ^{13}C O. Values in parentheses correspond to poorly resolved peaks and shoulders. They were used in the EFFF calculation with a statistical weight of 0.1 for the 1945 and 1805 cm^{-1} peaks and 0.5 for the one at 1972 cm^{-1} .

^b Identified as a well developed peak after subtracting the spectrum of the sample with ^{13}C O in natural abundance from the spectrum of the 16% ^{13}C O enriched sample.

Table 3 The EFFF CO stretching force constants (N m^{-1}) of $\text{Cr}(\text{CO})_4(\text{bpy})$ and the $[\text{Cr}(\text{CO})_4(\text{bpy})]^{-}$ radical anion

	$\text{Cr}(\text{CO})_4(\text{bpy})^a$	$[\text{Cr}(\text{CO})_4(\text{bpy})]^{-}$	Δk^b
k_{ax}	1513	1492	-21
k_{eq}	1419	1351	-68
$k_{\text{ax,ax}}$	64	83	+19
$k_{\text{eq,eq}}$	59	44	-15
$k_{\text{ax,eq}}$	42	32	-10

^a From ref. 32. ^b Difference between the force constants of the reduced and neutral complex. [Force constant values for the neutral and anionic species are based on IR spectra measured from 2-methyltetrahydrofuran and THF solutions, respectively. However, this should not affect the values obtained since the solvent effect on the $\nu(\text{CO})$ wavenumbers is negligible, comparable with the spectral resolution.]

Discussion

The EPR spectrum of $[\text{Cr}(\text{CO})_4(\text{bpy})]^{-}$ is characteristic of a complex containing a radical-anionic ligand co-ordinated to a metal atom with a low-spin d^6 electron configuration.¹ Values of $a(\text{H})$ and $a(\text{N})$ coupling constants are close to those reported^{12,17} for unco-ordinated $\text{bpy}^{\cdot-}$. An increase in the $a(\text{N})$ value from 17 0.241 to 0.3705 mT on going from $\text{bpy}^{\cdot-}$ to $[\text{Cr}(\text{CO})_4(\text{bpy})]^{-}$ points to a larger spin density on the nitrogen donor atoms in the complex ion. The $a(^{53}\text{Cr})$ value of 0.128 mT is rather small, corresponding to 0.56% of the A_{iso} value^{35,36} for Cr^0 . This indicates only a limited delocalisation of the unpaired electron density to the Cr atom.

Importantly, a sizeable hyperfine splitting due to the ^{13}C nuclei of the axial ^{13}C O ligands has been observed for the ^{13}C O-enriched $[\text{Cr}(\text{CO})_4(\text{bpy})]^{-}$. No evidence for the ^{13}C hfs from the equatorial CO ligands was found. The very existence of the two EPR-distinct CO positions in $[\text{Cr}(\text{CO})_4(\text{bpy})]^{-}$, with much larger coupling from the axial one, indicates that $[\text{Cr}(\text{CO})_4(\text{bpy})]^{-}$ keeps the geometry of a *cis*-disubstituted octahedron, ruling out any significant distortion of the $\text{Cr}(\text{CO})_4$ moiety. No interchange of CO ligands occurs on the EPR or faster time-scales.

The $^{13}\text{C}(\text{CO})$ coupling found for $[\text{Cr}(\text{CO})_4(\text{bpy})]^{-}$ is much larger than that measured^{38,39} for $[(\text{OC})_5\text{M}(\mu\text{-L})\text{M}(\text{CO})_5]^{-}$,

Table 4 Normal coordinates of Cr(CO)₄(bpy) and the [Cr(CO)₄(bpy)]⁻ radical anion^a

	Cr(CO) ₄ (bpy)] ⁻ ^b	Cr(CO) ₄ (bpy) ^c
Q(A ₁ ²)	0.673(r ₁ + r ₂) + 0.216(r ₃ + r ₄)	0.613(r ₁ + r ₂) + 0.353(r ₃ + r ₄)
Q(A ₁ ¹)	-0.216(r ₁ + r ₂) + 0.673(r ₃ + r ₄)	-0.353(r ₁ + r ₂) + 0.613(r ₃ + r ₄)
Q(B ₁)	1/√2(r ₁ - r ₂)	1/√2(r ₁ - r ₂)
Q(B ₂)	1/√2(r ₃ - r ₄)	1/√2(r ₃ - r ₄)

^a r₁ and r₂ stand for the C–O internal coordinates (bond lengths) in the axial CO ligands while r₃ and r₄ represent the equatorial ones, see Fig. 1.
^b This work. ^c From ref. 32.

M = Mo or W, L = radical anions of pyrazine or 4,4'-bpy, 0.07–0.12 mT. On the other hand, larger ¹³C(CO) couplings, from 0.84 to 1.12 mT, were found^{41,42} for Fe, Mn or Re carbonyl complexes of a bis(ethoxythiocarbonyl)sulfide radical-anionic ligand which forms a five-membered chelate ring. These species differ from [Cr(CO)₄(bpy)]⁻ in the symmetry of the singly occupied orbital and larger spin densities on the S-donor atoms.

The rather large value of the ¹³C(CO) coupling observed for [Cr(CO)₄(bpy)]⁻, 0.601 mT, is explained by the σ/π* hyperconjugation mechanism.^{1,8,36–40} This involves an interaction between the π*(bpy⁻) orbital and the C–Cr–C axial σ bonding and/or antibonding orbitals of b₁ symmetry. The latter are composed of an out-of-phase combination of the two lone electron pairs of the axial CO ligands, σ₁ and σ₂, which is in a bonding or antibonding interaction, respectively, with the Cr 4p_z orbital: σ = σ₁ - σ₂ + p_z; σ* = σ₁ - σ₂ - p_z. Their interaction with the singly occupied π*(bpy⁻) orbital results in a spin-polarisation of the electron density in the σ orbital and a delocalisation of the spin density from π*(bpy⁻) into the σ* orbital. It follows that the reduction of the bpy ligand affects the axial C–Cr–C σ bonding. This observation is in accordance with the labilisation of the axial Cr–CO bonds both in the reduced [Cr(CO)₄(bpy)]⁻ anion and MLCT-excited Cr(CO)₄(bpy), respectively.^{13,14}

An alternative π mechanism for the spin delocalisation to the axial CO ligands could involve a direct through-space overlap between π*(bpy⁻) and CO π* orbitals or their coupling through the Cr d_{xz} orbital. However, this π mechanism appears to be much less important than the σ/π* hyperconjugation. Comparison of the a(¹³C)/A_{iso}(¹³C) and a(³¹P)/A_{iso}(³¹P) ratios for [Cr(CO)₄(bpy)]⁻ and [Cr(CO)₃(PBUⁿ₃)(bpy)]⁻ of 0.54 and 0.96%, respectively, indicates that the transmission of the spin density to the axial ligands is ca. 1.8 times more efficient for the phosphine complex. This is most probably due to a better interaction between the π*(bpy⁻) orbital and the bonding and/or antibonding Cr–P σ orbitals which are closer in energy to the π*(bpy⁻) orbital than the Cr–C ones. Moreover, the π mechanism should be more efficient for the better π-accepting CO ligand than for PBUⁿ₃, contrary to the experiment. Also, hfs due to π delocalisation is known to be very small because of the lack of a direct involvement of atomic s orbitals.³⁶

The changes of the CO stretching force constants on going from Cr(CO)₄(bpy) to its radical anion allow us to assess separately the effects of the reduction on the axial and equatorial CO ligands. The stretching force constant of the equatorial CO ligands, k_{eq}, was found (Table 3) to fall by 68 N m⁻¹ while that of the axial CO ligands, k_{ax}, decreased by only 21 N m⁻¹. It may be estimated⁴³ that the axial and equatorial C≡O bonds lengthen on reduction by 0.003 (at most) and 0.009 Å, respectively. Obviously, the effect of the reduction of the bpy ligand in Cr(CO)₄(bpy) on the Cr(CO)₄ moiety is highly directional, directly mostly to the equatorial CO ligands.

On reduction, the bpy ligand changes from a weak π acceptor to a π donor. The interaction of the Cr d_{xz} orbital with the singly occupied π*(bpy⁻) orbital will, in turn, strengthen the d_{xz}→π*(CO) back donation. Here, π*(CO) is the lowest unoccupied symmetry-adapted orbital of the Cr(CO)₄ unit that has the right symmetry to interact with the d_{xz} orbital, i.e. b₁. Apparently, π*(CO) is composed mostly of

the in-phase combination of the π*(z) orbitals of the equatorial CO ligands, the contribution from the out-of-phase combination of the π*(x) orbitals of the axial CO's being much smaller. Increase of the back donation into such an orbital would clearly weaken the C≡O π bonds within the equatorial ligands much more than those in the axial CO ligands, in accordance with the experiment: Δk_{eq} = 3.2Δk_{ax}. Qualitatively, this effect may be viewed as a highly directional polarisation of the π-electron density along the x axis (i.e. C₂) toward the equatorial CO ligands. Interestingly, a decrease of the k_{eq} values, but not of the k_{ax} ones, occurs⁴⁴ between Cr(CO)₄(RN=CHCH=NR) (R = aryl) and Cr(CO)₄(R'N=CHCH=NR') (R' = alkyl) while the π-acceptor strength of the diazabutadiene ligand diminishes. In addition, other effects like an increase in the N→Cr σ donation or a π donation from low-lying occupied π orbitals of bpy⁻ may also contribute to the decrease of both k_{ax} and k_{eq} on the reduction.

Finally, it should be noted that the conventional model^{26–28} of the relations between the CO stretching force constants and the π-back bonding would predict Δk_{eq} = 0.5Δk_{ax}. This is because the overlap between d_{xz} and the π*(x) orbitals of the axial CO's is about twice the overlap with the π*(z) orbitals of the equatorial CO ligands. This prediction is in an obvious contradiction with the experiment as was first recognised by Dessy and Wiczorek.¹² It was suggested that directional σ polarisation might be responsible. However, the *trans* labilisation of the Cr–(CO)_{eq} σ bonds due to increased ligand basicity on going from bpy to bpy⁻ can hardly account for the dramatic drop in k_{eq} because of a mutual compensation of resulting σ and π effects on the C≡O bonding.^{45,46} Also, the *trans* σ influence on ν(CO) wavenumbers is usually rather small.⁴⁷ Moreover, no chemical labilisation of the equatorial Cr–CO bonds in Cr(CO)₄(bpy) was observed on reduction or MLCT excitation. Above, we have shown, that the observed changes of the CO stretching force constants may be satisfactorily explained by the preferential π-back bonding to the equatorial CO ligands, without invoking σ effects.

Conclusion

The reduction of Cr(CO)₄(bpy) to [Cr(CO)₄(bpy)]⁻ is predominantly localised on the bpy ligand. Molecular structures of both Cr(CO)₄(bpy) and [Cr(CO)₄(bpy)]⁻ are virtually identical. Comparison of the CO stretching force constants for Cr(CO)₄(bpy) and [Cr(CO)₄(bpy)]⁻ and the magnitude of the ¹³C(CO) EPR hyperfine splitting found for [Cr(CO)₄(bpy)]⁻ indicate that the reduction of the co-ordinated bpy ligand to bpy⁻ induces significant redistribution of the electron density within the Cr(CO)₄ moiety. Two main effects of the reduction were found.

First, there is a small delocalisation of the spin density from the bpy⁻ ligand to the C atoms of the axial CO ligands. It originates in an interaction between the singly occupied π* orbital of the bpy⁻ ligand and the axial C–Cr–C σ bonding and/or antibonding orbitals. This effect could account for the known labilisation of the axial Cr–CO bonds upon reduction or MLCT excitation of Cr(CO)₄(bpy). Interestingly, no spin delocalisation occurs to the equatorial CO ligands which lie in the nodal plane of the bpy π system.

Second, the π -electron density in the $\text{Cr}(\text{CO})_4$ fragment of the $[\text{Cr}(\text{CO})_4(\text{bpy})]^-$ anion appears to be strongly polarised toward the equatorial CO ligands. Reduction of $\text{Cr}(\text{CO})_4(\text{bpy})$ to the $[\text{Cr}(\text{CO})_4(\text{bpy})]^-$ anion strengthens the π -back donation to the equatorial CO ligands much more than to the axial ones. This conclusion agrees well with both the electrochemical¹⁸ and photochemical²⁴ stability of equatorial Cr–C bonds in $\text{Cr}(\text{CO})_4(\text{bpy})$.

Acknowledgements

Financial support from the European Cooperation in the field of Scientific and Technical Research (COST) D4 Action and from the European Science Network 'Organometallic Photochemistry' is gratefully appreciated. J. W. H. Peeters and R. Fokkens of the Inst. of Mass Spectrometry, University of Amsterdam, and V. Hanuš, J. Heyrovský Inst., are thanked for determining the isotopic composition of the ¹³C-enriched samples.

References

- W. Kaim, *Coord. Chem. Rev.*, 1987, **76**, 187.
- A. Vlček, jun., *Chemtracts: Inorg. Chem.*, 1993, **5**, 1 and refs. therein.
- K. C. Gordon, A. H. R. Al-Obaidi, P. M. Jayaweera, J. J. McGarvey, J. F. Malone and S. E. J. Bell, *J. Chem. Soc., Dalton Trans.*, 1996, 1591.
- A. H. R. Al-Obaidi, K. C. Gordon, J. J. McGarvey, S. E. J. Bell and J. Grimshaw, *J. Phys. Chem.*, 1993, **97**, 10 942.
- Y. F. Lee, J. R. Kirchhoff, R. M. Berger and D. Gosztola, *J. Chem. Soc., Dalton Trans.*, 1995, 3677.
- O. Kahn, *Molecular Magnetism*, VCH, New York, 1993.
- F. Hartl and A. Vlček, jun., *Inorg. Chem.*, 1996, **35**, 1257.
- A. Klein, C. Vogler and W. Kaim, *Organometallics*, 1996, **15**, 236.
- D. M. Schut, K. J. Keana, D. R. Tyler and P. H. Rieger, *J. Am. Chem. Soc.*, 1995, **117**, 8939.
- F. Mao, D. R. Tyler, M. R. M. Bruce, A. E. Bruce, A. L. Rieger and P. H. Rieger, *J. Am. Chem. Soc.*, 1992, **114**, 6418.
- F. Mao, D. R. Tyler and D. Keszler, *J. Am. Chem. Soc.*, 1989, **111**, 130.
- R. E. Dessy and L. Wiczorek, *J. Am. Chem. Soc.*, 1969, **91**, 4963.
- D. Miholová, B. Gaš, S. Zális, J. Klíma and A. A. Vlček, *J. Organomet. Chem.*, 1987, **330**, 75.
- J. Vichová, F. Hartl and A. Vlček, jun., *J. Am. Chem. Soc.*, 1992, **114**, 10 903.
- Y. Kaizu and H. Kobayashi, *Bull. Chem. Soc. Jpn.*, 1970, **43**, 2492.
- Y. Kaizu and H. Kobayashi, *Bull. Chem. Soc. Jpn.*, 1972, **45**, 470.
- W. Kaim, *Chem. Ber.*, 1981, **114**, 3789.
- D. Miholová and A. A. Vlček, *J. Organomet. Chem.*, 1985, **279**, 317.
- R. W. Balk, T. Snoeck, D. J. Stufkens and A. Oskam, *Inorg. Chem.*, 1980, **19**, 3015.
- D. M. Manuta and A. J. Lees, *Inorg. Chem.*, 1986, **25**, 1354.
- S. Wieland, K. Bal Reddy and R. van Eldik, *Organometallics*, 1990, **9**, 1802.
- F. Wen-Fu and R. van Eldik, *Inorg. Chim. Acta*, 1996, **251**, 341.
- A. Vlček, jun., J. Vichová and F. Hartl, *Coord. Chem. Rev.*, 1994, **132**, 167.
- I. G. Virrels, M. W. George, J. J. Turner, J. Peters and A. Vlček, jun., *Organometallics*, 1996, **15**, 4089.
- D. Guillaumont, C. Daniel and A. Vlček, jun., *Inorg. Chem.*, 1997, **36**, 1684.
- P. S. Braterman, *Metal Carbonyl Spectra*, Academic Press, London, 1975.
- F. A. Cotton and C. S. Kraihanzel, *J. Am. Chem. Soc.*, 1962, **84**, 4432.
- C. S. Kraihanzel and F. A. Cotton, *Inorg. Chem.*, 1963, **2**, 533.
- F. A. Cotton, *Inorg. Chem.*, 1964, **3**, 702.
- J. K. Burdett, M. Poliakoff, J. A. Timney and J. J. Turner, *Inorg. Chem.*, 1978, **17**, 948.
- M. H. B. Stiddard, *J. Chem. Soc.*, 1962, 4712.
- A. Vlček, jun., F. W. Grevels, T. L. Snoeck and D. J. Stufkens, *Inorg. Chim. Acta*, in the press.
- F. Hartl, H. Luyten, H. A. Nieuwenhuis and G. C. Schoemaker, *Appl. Spectrosc.*, 1994, **48**, 1522.
- H. tom Dieck, K.-D. Franz and F. Hohmann, *Chem. Ber.*, 1975, **108**, 163.
- B. A. Goodman and J. B. Raynor, *Adv. Inorg. Chem. Radiochem.*, 1970, **13**, 135.
- M. Symons, *Chemical and Biological Aspects of Electron-Spin Resonance Spectroscopy*, Van Nostrand Reinhold, Wokingham, 1978.
- F. Hartl and A. Vlček, jun., *Inorg. Chem.*, 1991, **30**, 3048.
- W. Kaim, *Chem. Ber.*, 1982, **115**, 910.
- W. Kaim, *Inorg. Chim. Acta*, 1981, **53**, L151.
- W. Kaim and S. Kohlmann, *Inorg. Chem.*, 1990, **29**, 2909.
- W. G. McGimpsey, M. C. Depew and J. K. S. Wan, *Organometallics*, 1984, **3**, 1684.
- A. Alberti, M. C. Depew, A. Hudson, W. G. McGimpsey and J. K. S. Wan, *J. Organomet. Chem.*, 1985, **280**, C21.
- S. L. Morrison and J. J. Turner, *J. Mol. Struct.*, 1994, **317**, 39.
- H. tom Dieck, T. Mack, K. Peters and H.-G. von Schnering, *Z. Naturforsch., Teil B*, 1983, **38**, 568.
- J. T. Poulton, M. P. Sigalas, K. Folting, W. E. Streib, O. Eisenstein and K. G. Caulton, *Inorg. Chem.*, 1994, **33**, 1476.
- K. S. Wang, D. Wang, K. Yang, M. G. Richmond and M. Schwartz, *Inorg. Chem.*, 1995, **34**, 3241.
- R. J. Angelici and M. D. Malone, *Inorg. Chem.*, 1967, **6**, 1731.

Received 8th August 1997; Paper 7/05819E